

Far-infrared reflection spectra of $1T\text{-TaS}_2$ and $1T\text{-TaSe}_2$ in commensurate and incommensurate charge-density-wave states

D. R. Karecki and B. P. Clayman

Department of Physics, Simon Fraser University, Burnaby, British Columbia V5A 1S6, Canada

(Received 6 November 1978)

Ten strong infrared-active modes have been observed in both $1T\text{-TaS}_2$ and $1T\text{-TaSe}_2$ in their commensurate charge-density-wave (CDW) states. The frequency ratios of corresponding modes in the two crystals indicate that the four low-frequency and six high-frequency modes arise from the acoustic- and optic-phonon branches, respectively, of the undistorted crystal folded into $k = 0$ modes by the CDW-induced lattice distortion. In $1T\text{-TaSe}_2$, a strong absorption is observed, corresponding to each mode, as the temperature is lowered to 4.2 K. This appears to be related to a strong scattering of the charge carriers responsible for most of the reflectivity at each phonon frequency.

I. INTRODUCTION

An electronic instability, known as a charge-density wave (CDW), appears in the almost two-dimensional layered compounds $1T\text{-TaS}_2$ and $1T\text{-TaSe}_2$. The electrostatic forces generated by the CDW cause a structural deformation of the lattice known as a periodic structural distortion (PSD). Structural details have been well documented by neutron, x-ray, and electron-diffraction studies.¹⁻³

At temperatures below 180 K in $1T\text{-TaS}_2$ and 473 K in $1T\text{-TaSe}_2$, the periodicity of the CDW is such that it is commensurate with the CdI_2 -type host lattice and forms a larger unit cell. This supercell is triclinic with a $\sqrt{13}a_0 \times \sqrt{13}a_0$ basal plane and one layer thickness. Adjacent atoms are stacked as reported by Moncton *et al.*² There are 39 atoms in the new unit cell of this "commensurate" phase.

Above 370 K in $1T\text{-TaS}_2$ and 473 K in $1T\text{-TaSe}_2$, the CDW distortion is not periodic with the lattice. This is called the "incommensurate" phase. In between about 220 and 350 K in $1T\text{-TaS}_2$ the CDW distortion becomes very close to that of the commensurate state, locking in at the transition temperature. This is referred to as the "quasicommensurate" phase. The temperatures of the phase transitions of both crystals exhibit a degree of hysteresis.

That the CDW distortion drastically alters the Fermi surface can be seen in the behavior of the electrical conductivity of both crystals. At the 473-K structural phase transition in $1T\text{-TaSe}_2$, the dc conductivity abruptly drops from $\sigma_0 \cong 2500$ mho/cm in the incommensurate phase to $\sigma_0 \cong 500$ mho/cm in the commensurate phase. In $1T\text{-TaS}_2$ at 350 K the conductivity drops from $\sigma_0 \cong 2000$ mho/cm in the incommensurate phase to $\sigma_0 \cong 1000$ mho/cm in the quasicommensurate phase. At

180 K it then drops from about 300 mho/cm to 20 mho/cm.

Both the unusual structural and electrical properties caused by the CDW affect the observed far-infrared and Raman spectra of these crystals. Many optically active phonon modes are observed due to the large size of the unit cell in the commensurate phase.⁴⁻⁷ These can, in principle, be related to the phonon spectrum of the undistorted lattice. The charge carriers associated with electrical conductivity contribute to a high overall reflectivity with distinct jumps at the transition temperatures.^{4,5} They also screen out the phonon modes to a great extent in the case of $1T\text{-TaSe}_2$,⁵ and to a lesser extent in the case of $1T\text{-TaS}_2$ in the commensurate phase.⁴ This is expected from the values of their dc conductivities.

This paper contains the complete far-infrared reflection spectra of both $1T\text{-TaS}_2$ and $1T\text{-TaSe}_2$ in the commensurate state. Other observations are made which should prove useful in understanding the phonon spectra of these materials and how they are influenced by the CDW.

II. EXPERIMENT

The samples used in this experiment were single crystals grown by the iodine vapor transport method. Following growth, the hot quartz sample tubes were plunged into water to quench the crystals into the metastable $1T$ phase.

In order to characterize the crystals more fully, the dc resistance versus temperature was measured. Phase transitions occurred at the expected temperatures for both crystals. The absolute conductivity is difficult to determine because the crystals are small, not of uniform thickness, and the contact size is not negligible. At room temperature, different crystals of $1T\text{-TaS}_2$ grown by different workers seem to have similar conductiv-

ity.⁸ Normalizing our room-temperature resistance value to agree with their results gives $\sigma_0 = 70 \pm 7$ mho/cm at 100 K for the crystals used.

A composite sample of several large (~ 0.25 cm²) 1T-TaS₂ crystals was constructed for the reflectivity measurements. Al foil pressed over the surface served as a reference. Al is almost perfectly reflecting in the far infrared. Any geometrical effects caused by the composite sample should divide out when the ratio of the sample spectrum to reference is taken.

One large single crystal of 1T-TaSe₂ was studied in reflection. To bring out the very weak structure observed in a single bounce, a dual cavity technique was also used.⁹ In this technique, light is introduced into a sample-lined cavity through a small hole and makes a number of reflections before exciting to the detector. In the case of 1T-TaSe₂, many reflections are made because of its high reflectivity. An identical polished brass cavity served as a reference.

Spectra were obtained with a modified Beckman FS-720 Fourier spectrometer as energy source and analyzer. Brass light pipes 1.2 cm in diameter directed the light to the samples and the detector. For frequencies below 250 cm⁻¹ the detector was a doped Ge bolometer operating at 0.3 K. A Si bolometer at 4.2 K was used for higher frequencies where the quartz window of the 0.3-K detector blocks the radiation.

III. RESULTS

As reported earlier,⁴ the spectra of 1T-TaS₂ in the incommensurate and quasicommensurate phases were observed to be featureless, the re-

fectivity decreasing slightly with frequency. The reflectivity decreased by 4% at the transition into the quasicommensurate phase, and by 15% upon entry into the commensurate phase. Very little temperature dependence of the reflectivity in the commensurate phase was observed. The spectrum at 100 K and 15° incidence is presented in Fig. 1. In addition to the modes previously reported,⁴ there are modes extending out to almost 400 cm⁻¹.

The single reflection measurements taken on 1T-TaSe₂ at 4.2, 100, and 295 K show that even the strongest spectral features are difficult to separate from the background noise. At the two higher temperatures the features were only 1%, or less, of the total reflectivity, while at 4.2 K they were perhaps 3%. The more detailed multi-reflection spectra taken with the dual cavity are shown in Fig. 2. The absolute magnitude of the ratios were reproducible only to $\pm 20\%$, between data taken in different experiments. This is most likely due to difficulty in aligning the apparatus in which the cavities had to be rotated into the sample beam. At 100 and 295 K, low- and high-frequency results were matched at about 90 cm⁻¹ to form the complete spectra shown in Fig. 2.

These spectra exhibit several features of interest. At 100 K, a small dip in the reflectivity can be seen developing just above the estimated TO frequency of each mode at room temperature. By 4.2 K, these dips become very pronounced for the high-frequency modes but are barely discernible for the lower-frequency modes.

At 295 K, in addition to the modes reported by Lucovsky *et al.*,⁵ four low-frequency modes appear. As the temperature was raised to 500 K, a small rise in the transmission through the cavity was

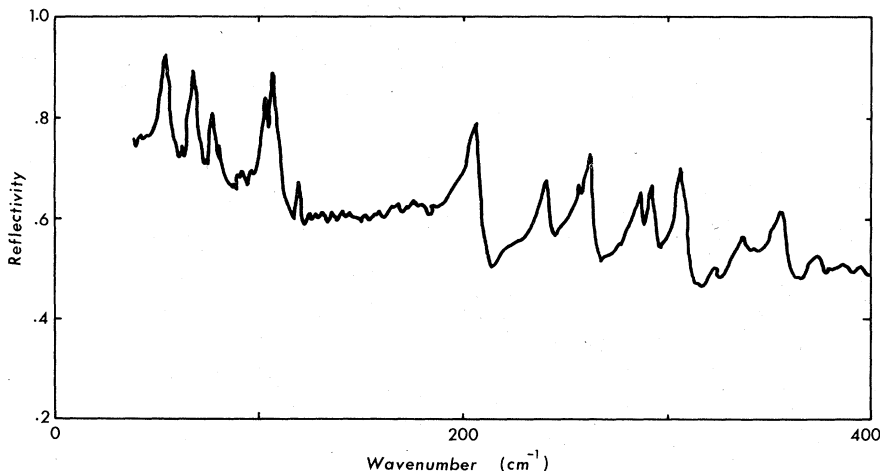


FIG. 1. Reflectivity of 1T-TaS₂ at 100 K and 15° incidence. Resolution is 2 cm⁻¹ above 200 cm⁻¹ and 1 cm⁻¹ below 200 cm⁻¹.

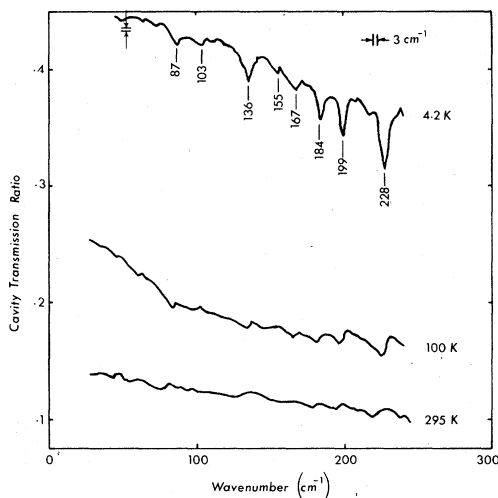


FIG. 2. Ratio of intensity transmitted through a cavity lined with 1T-TaS₂ to that transmitted through a polished brass cavity at 4.2, 100, and 295 K.

noted (about 3%), but no spectral structure was observed in the incommensurate state.

To check for very low frequency modes, measurements were taken on both crystals down to ~ 2 cm⁻¹. Because the wavelengths become equal to the size of irregularities in the sample, a rise in reflection was observed that was not due to the intrinsic reflectivity of the sample. No structure attributable to phonons was observed.

IV. DISCUSSION

Wilson³ has recently discussed the structural changes caused by the CDW in the commensurate phases of 1T-TaS₂ and 1T-TaSe₂. In 1T-TaS₂, the Ta-Ta separation is reduced by 7% for 13 atoms surrounding each corner of the supercell. Furthermore, the amplitude of the CDW is such that approximately a full charge has been added to the corner Ta atom. These are major changes and must affect the force constants and dipole moments associated with the lattice motion responsible for infrared activity.

A more complete description is difficult. The space group of this new supercell has not been reported. Until it is known, a group-theoretical analysis of the $k=0$ modes cannot be made. Furthermore, the determination of the phonon dispersion curves by neutron scattering has not been done. In the quasicommensurate phase of 1T-TaS₂ at room temperature, part of the acoustic branch of the phonon-dispersion curves has been determined,¹⁰ enough to see a Kohn anomaly in the acoustic LA phonon but not enough to determine the zone-edge frequencies. It should be mentioned that the small volume of available crystals makes these measurements difficult.

TABLE I. Fitting parameters for 1T-TaS₂ at 100 K.

$\bar{\nu}_0$ (cm ⁻¹)	S	τ (10 ¹² sec)
54	2.3	3.1
68	9.6	2.8
78	4.7	1.1
104	5.7	1.9
107	2.1	5.4
204	2.4	1.5
241	0.66	1.8
256	0.52	1.0
261	0.89	1.4
286	0.41	1.6
292	0.51	1.4
306	0.76	1.3
355	0.57	0.8

In order to determine the frequencies of the phononmodes, the observed reflection spectrum for 1T-TaS₂ (Fig. 1) was fit with a number of Lorentz oscillators plus one Drude term. The following expression was used for the dielectric constant:

$$\epsilon = \epsilon_{\infty} + \sum_{j=1}^N \frac{S_j \bar{\nu}_j^2}{\bar{\nu}_j^2 - \bar{\nu}^2 - i\bar{\nu}/2\pi c\tau} - \frac{\bar{\nu}_p^2}{\bar{\nu}(\bar{\nu} + iG)}$$

The Drude parameters for the free carriers, $\bar{\nu}_p$ and G , were allowed to vary separately, although only the ratio $\bar{\nu}_p^2/G$ was likely to be important. Although 19 oscillators were used in the fit, only the ones with large strengths are included in the summary of results in Table I. The weaker ones are omitted because the quality of the fit was not sensitive to their precise values. The reflectivity calculated from the fit is the solid line in Fig. 3. The conductivity deduced from the fitting parameters extrapolated at low frequencies to 67 mho/cm, agreeing well with the dc value found above.

TABLE II. Dominant phonon frequencies in cm⁻¹ and their ratios. The frequencies in parentheses are those of Lucovsky *et al.*⁵

TaS ₂	TaSe ₂	$\bar{\nu}(\text{TaS}_2)/\bar{\nu}(\text{TaSe}_2)$
54	45	1.20
68	60	1.13
78	81	0.96
104	98	1.06
107		1.09
204	135 (135.1)	1.51
241	153 (152.8)	1.58
256	165 (165.4)	1.55
261		1.58
286	182 (182.3)	1.57
292		1.60
306	197 (196.7)	1.55
355	225 (224.9)	1.58

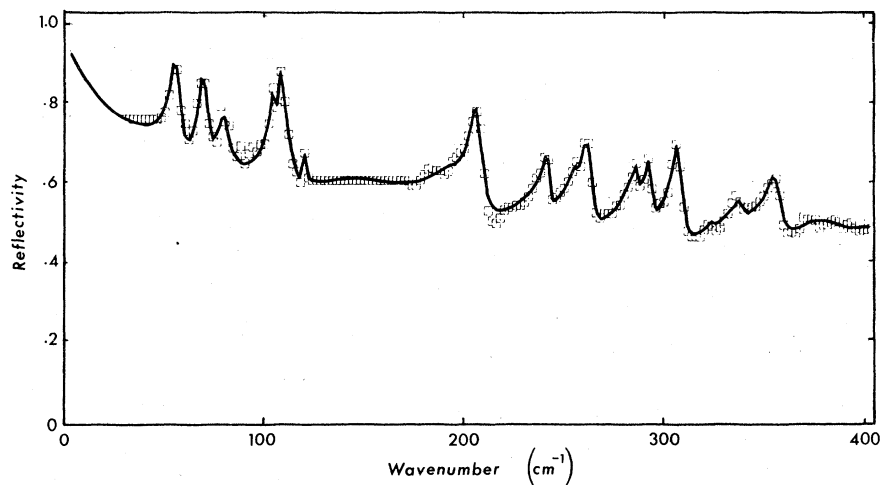


FIG. 3. Oscillator fit to $1T\text{-TaS}_2$ reflectivity at 100 K. Squares are experimental values.

In addition to the oscillator fit, a Kramers-Kronig¹¹ analysis of the spectrum of $1T\text{-TaS}_2$ was performed. Low frequencies were extrapolated using the above oscillator fit. The data of Barker¹² were used for frequencies above 500 cm^{-1} , although a constant reflectivity extrapolation at high frequencies gave similar results. The transverse-optical frequencies so obtained agreed within 1 cm^{-1} with the frequencies obtained from the oscillator fit. The constants n and k agreed within 20% with those generated from the oscillator fit over the frequency range of the modes.

Because of the ranges of angles of incidence and unknown number of reflections in the cavity, no such analysis could be made of the $1T\text{-TaSe}_2$ spectrum shown in Fig. 2. However, a spectrum generated from oscillator parameters similar to those used in the above fit and Drude parameters deduced from the dc conductivity together with a cavity model of Tinkham and Richards¹³ resembles the spectrum of Fig. 2 at 295 K. The transverse-optical frequencies should be at the leading edge of each reflectivity peak and were estimated to within 2 cm^{-1} from the room-temperature spectrum. The six higher frequencies agreed with the results of Lucovsky *et al.*⁵ Table II lists the results.

The spectra of Figs. 1 and 2 have regions of low- and high-frequency modes separated by featureless gaps. Ignoring small details on the $1T\text{-TaS}_2$ spectra, a correspondence between modes in the two systems can be made which is summarized in Table II. Since the crystal structures of the two crystals are identical, the number of modes should be the same. The fact that the oscillator strengths used in the fit of $1T\text{-TaSe}_2$ by Lucovsky *et al.*⁵ correspond well with the $1T\text{-TaS}_2$ parameters given here further confirms that the

modes are matched correctly.

The zone center of the superlattice has phonons folded into it from $k \neq 0$ modes of the undistorted crystal at the distortion wave vector. For the $1T\text{-TaS}_2$ superlattice, the distortion wave vector is not at the zone edge nor does it lie along a direction of high symmetry. A full analysis is difficult.

A qualitative understanding can be gained by considering a linear chain model of the original three-atom unit cell. For an optic mode with the two anions moving in phase, the ratio $\bar{\nu}(\text{TaSe}_2)/\bar{\nu}(\text{TaS}_2)$ of mode frequencies in the two crystals would be 1.34 at the zone center and 1.57 at the zone edge if the force constants were identical. The cation is at rest in the zone-edge mode. For an acoustic mode, the ratio at the zone edge is unity since the anion is at rest and would increase towards the zone center tending to 1.18 at $k=0$.

The frequency ratios have been taken for the modes in Table II and are listed there. The six high-frequency modes have ratios close to the inverse square root of the Se-S mass ratio, 1.57. This suggests that the heavier Ta atom is almost at rest in these modes, and that they are probably derived from optic modes of the undistorted crystal.

For the four low-frequency modes, the ratio lies between 0.96 and 1.20. This is below the ratio predicted for optic modes by the simple model above but in qualitative agreement with those predicted for acoustic modes. Of course the actual frequencies are lower, as would be expected for acoustic modes. The gap between the low- and high-frequency modes corresponds to the gap between acoustic and optic bands.

Figure 2 shows that there exists a strong temperature dependence for the reflectivity of

1T-TaSe₂ in the commensurate phase. As the temperature is lowered, a dip in the reflectivity is observed at a frequency slightly higher than the estimated transverse-optical frequency of each mode. The dips are much more pronounced for the six high-frequency modes.

These dips in the spectrum of Fig. 2 at 4.2 K correspond to a sharp absorption by the crystals. Only a very strong temperature dependence of the oscillator fitting parameters would generate such behavior. This is difficult to justify physically. The increased conductivity of 1T-TaSe₂ should, in fact, screen out the modes even more than is the case at 295 K. It is more likely that the carriers responsible for most of the reflectivity are strongly scattered at this frequency by an interaction with the phonons the details of which are unknown.

The phonon mode at 210 cm⁻¹ observed by Lucovsky *et al.*⁵ in 1T-TaS₂ at 295 K was not seen here either in a single reflection or in the dual cavity. It is possible that our crystals were off-stoichiometry, having an excess of Ta. This excess would increase the number of carriers screening out the phonon modes in reflection. dc measurements of the crystals used here suggest this possibility as their low-temperature conductivity is higher than that of the best crystals, as reported by others.⁸

So far no attempt has been made to describe all the modes seen in the more detailed 1T-TaS₂ spectrum. The Kramers-Kronig analysis yielded as many as 31 modes. The weaker modes and side structure on the strong modes could be due to impurities, higher-order combinations, or even weak $k=0$ fundamental modes.

While definite assignment cannot be made it is interesting to compare the present infrared work on 1T-TaS₂ with the Raman spectrum obtained by Duffey *et al.*⁶ Mode activity is restricted to the same high- and low-frequency bands. In the low-frequency region (50–140 cm⁻¹), 17 ir and 12

Raman modes can be matched to within 3 cm⁻¹. In the high-frequency region (200–400 cm⁻¹), there is no counterpart of the 204 cm⁻¹ ir-active mode in the Raman spectrum. In the same region, the other 14 ir modes differ in frequency by up to 15 cm⁻¹ from the frequency of the 18 observed Raman modes.

No one-to-one mode correspondence between the ir and Raman modes has been attempted here. A large number of accidental degeneracies is to be expected when so many modes occur close together. Only if the modes were assigned the symmetry elements of the irreducible representations of the space group at $k=0$ could a statement be made regarding the degeneracy between ir and Raman modes having the same symmetry.

V. SUMMARY

Ten strong ir-active phonon modes have been found in the commensurate CDW phase of both 1T-TaS₂ and 1T-TaSe₂. These seem to be related to the acoustic and optic branches of the undistorted unit cell now folded into $k=0$ modes by the strong distortion of the lattice by CDW's, and the consequent formation of a larger unit cell. Little temperature dependence of the mode frequency in the commensurate (CDW) phase was seen. However, below 295 K in the 1T-TaSe₂, a strong dip in the reflectivity, due to an absorption process, was observed near the transverse-optical phonon frequency of each mode. This is suggestive of a strong interaction between the free carriers and phonons, perhaps mediated by collective modes of the CDW's themselves. Further work is being carried out to explore this possibility.

ACKNOWLEDGMENTS

We acknowledge helpful discussions with Dr. J. C. Irwin and the support of the National Science and Engineering Research Council of Canada.

¹C. B. Scruby, P. M. Williams, and G. S. Parry, *Philos. Mag.* **31**, 255 (1975).

²D. E. Moncton, F. J. DiSalvo, J. D. Axe, L. J. Sham, and Bruce R. Patton, *Phys. Rev. B* **14**, 3432 (1976).

³J. A. Wilson, *Phys. Rev. B* **17**, 3880 (1978).

⁴D. R. Karcicki and B. P. Clayman, *Solid State Commun.* **19**, 479 (1976).

⁵G. Lucovsky, W. Y. Liang, and R. M. White, *Solid State Commun.* **19**, 303 (1976).

⁶J. R. Duffey, R. D. Kirby, and R. V. Coleman, *Solid State Commun.* **20**, 617 (1976).

⁷J. C. Tsang, J. E. Smith, Jr., and M. W. Shafer, *Phys. Rev. B* **16**, 4239 (1977).

⁸F. J. DiSalvo and J. E. Graebner, *Solid State Commun.* **23**, 825 (1977); A. H. Thompson, F. R. Gamble, and J. F. Revelli, *ibid.* **9**, 981 (1971); J. P. Tidman and R. F. Frindt, *Can. J. Phys.* **54**, 2306 (1976).

⁹R. W. Ward, *Infrared Phys.* **16**, 385 (1976).

¹⁰K. R. A. Ziebeck, B. Dorner, W. G. Stirling, and R. Schollhorn, *J. Phys. F* **7**, 1139 (1977).

¹¹I. F. Chang, S. S. Mitra, J. N. Plendl, and L. C. Mansur, *Phys. Status Solidi* **28**, 663 (1968).

¹²A. S. Barker (private communication).

¹³P. L. Richards and M. Tinkham, *Phys. Rev.* **119**, 575 (1960).